AMERICAN SOCIETY FOR MICROBIOLOGY | Applied and Environmental Microbiology®

ENVIRONMENTAL MICROBIOLOGY

A Novel Whole-Cell Biosensor for Bioavailable Antimonite in Water and Sediments

Lixin Zhang,[a,b] Li Ye,[c] Chuanyong Jing[a,b,c]

[a]State Key Laboratory of Environmental Chemistry and Ecotoxicology, Research Center for Eco-Environmental Sciences, Chinese Academy of Sciences, Beijing, China
[b]University of Chinese Academy of Sciences, Beijing, China
[c]School of Environmental Science and Engineering, Shandong University, Qingdao, China

ABSTRACT Antimony (Sb) is an emerging contaminant, and its on-site speciation analysis is central to the accurate evaluation of its bioavailability and toxicity. The whole-cell biosensors (WCBs) for Sb(III) are promising but challenging due to the lack of Sb(III)-specific recognition components. Here, we constructed a novel Sb(III)-specific WCB using an Sb(III) transcriptional regulator (*antR*) and its cognate promoter (P_{ant}). To prevent the promoter leakage of P_{ant}, an additional regulatory gene, *antR*, was inserted downstream of the Sb(III)-inducible promoter, improving the sensitivity of the WCB by an order of magnitude and reaching the detection limit at 0.009 μM, which is lower than the WHO drinking water standard of Sb. Moreover, the WCB with double *antR* showed a high specificity toward Sb(III) compared with interfering ions at 3 orders of magnitude higher concentrations. This WCB was capable of measuring Sb(III) bioavailability in natural waters and sediments on-site, and its results were not statistically different from the chemical analysis. The insights gained from this work demonstrate that the addition of regulatory genes prevents promoter leakage and improves the sensitivity of WCBs in field applications.

IMPORTANCE Antimony (Sb) is a redox-sensitive pollutant ubiquitous in the environment. Sb(III) is dominant in the subsurface and is readily oxidized to less toxic Sb(V) upon exposure to air, and therefore, on-site Sb speciation analysis is essential to evaluate its bioavailability and toxicity. Dissolved Sb concentration and speciation can be determined accurately using on-site chemical sensors, but chemical sensors have difficulty determining the bioavailable Sb(III) that is taken up by the cells. Here, we constructed an Sb(III)-specific whole-cell biosensor (WCB) using double Sb(III) transcriptional regulators (*antR*) downstream of its cognate promoter P_{ant}. With an additional *antR*, the sensitivity of the WCB was improved by approximately 10 times, and the promoter leakage commonly found in WCBs was inhibited. Integrated with a tea-bag design, the WCB is able to measure Sb(III) bioavailability in natural water and sediments on-site. This study demonstrates the importance of inserting one more regulatory gene to improve sensitivity.

KEYWORDS antimony, whole-cell biosensor (WCB), Sb(III) transcriptional repressors (*antR*), promoter leakage, bioavailable Sb(III)

Antimony (Sb) is garnering public concern due to increased awareness of its toxicity, even at the trace level (1). Antimony interferes with sugar and protein metabolism, thereby damaging the heart, kidney, liver, and nervous system (1, 2). The rapid increase in industrial mineral exploration and extraction over the past decades has promoted Sb release into the aquatic environment (3–5). Antimony usually exists as Sb(III) oxyanions in the subsurface and would readily oxidize to less toxic Sb(V) upon exposure to air (6). Therefore, on-site Sb speciation analysis is essential for evaluating its bioavailability and toxicity.

The urgent need for monitoring Sb(III) on-site has motivated recent research on developing sensitive and rapid methods using chemical (7), electrochemical (8), and aptamer-based (9) sensors. However, only a fraction of Sb(III) in soils and sediments is bioavailable

Editor Jennifer B. Glass, Georgia Institute of Technology

Address correspondence to Chuanyong Jing, cyjing@rcees.ac.cn.

The authors declare no conflict of interest.

Received 24 October 2022
Accepted 7 December 2022
Published 5 January 2023

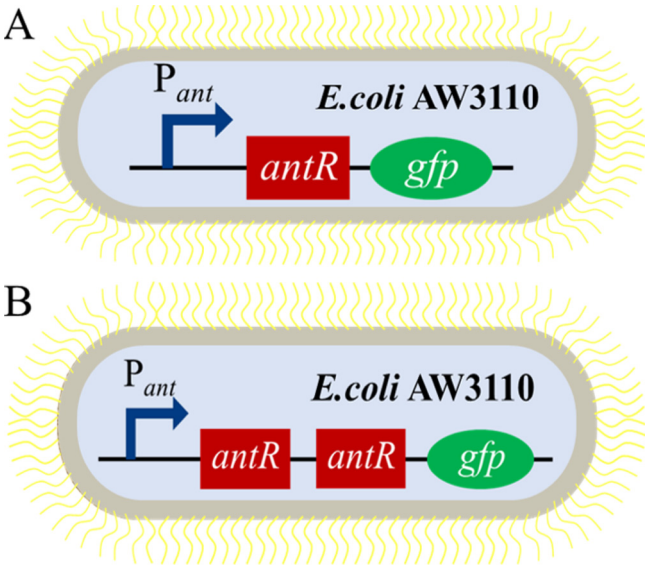

FIG 1 Schematic of the Sb(III) whole-cell biosensors (WCBs) with one *antR* (A) and two *antR*s (B).

(10, 11), and accurately identifying the bioavailable Sb(III) presents a contemporary challenge. Mounting evidence suggests that whole-cell biosensors (WCBs) are promising for field detection of bioavailable heavy metal(loid)s (10, 12), with the advantage of high sensitivity, strong specificity, and cost-effectiveness (11, 13).

Taking advantage of synthetic biology, the WCBs are realized by linking the recognition components, including transcriptional regulators and their cognate promoters (13), to the reporter unit, such as luciferase (14), *lacZ* (15), and fluorescent protein (16). The recognition components specifically recognize target metals and then turn on the expression of reporter genes. Thus, the targets can be quantified by measuring the signal intensity of the reporter unit (10, 13). The WCBs for arsenite, the analog for Sb(III), have been established successfully with the arsenic (As)-specific binding protein ArsR (12, 14). However, ArsR is unable to provide sufficient specificity and sensitivity for Sb(III) (17). Recently, the transcriptional regulator *antR* has been reported to specifically recognize Sb(III) (18, 19), facilitating our WCB construction for Sb(III).

Despite the advantages of WCBs and their successful proof of concept in the laboratory, the progress toward field applications has been hindered. Especially, the sensitivity usually suffers from promoter leakage (11, 13), and the complex environmental matrix may interfere with detection (11, 16). This study aimed to construct a WCB for on-site Sb(III) detection. To alleviate the promoter leakage commonly found in the WCBs, we inserted double *antR* genes downstream of the Sb(III)-inducible promoter P_{ant}. The sensitivity with double *antR* genes was increased by an order of magnitude and reached the Sb(III) detection limit at 0.009 μM. To avoid interference with the detection of the fluorescent signal, a semipermeable membrane was used to separate the cells from the suspension. This study provides the first WCB for bioavailable Sb(III) detection and demonstrates the importance of inserting one more regulatory gene to improve sensitivity, precision, and accuracy.

RESULTS

Proof of concept for Sb(III) whole-cell biosensor. To construct the whole-cell biosensor (WCB) for bioavailable Sb(III) analysis, the recombinant plasmid with one or two transcriptional regulators (*antR*) was transformed separately into *Escherichia coli* AW3110. As shown in Fig. 1A, an Sb(III) transcriptional regulator (*antR*), its cognate promoter (P_{ant}), and the reporter gene *gfp* were inserted into a plasmid pUC57, namely, pUC57-P_{ant}-*antR-gfp* (3,623 bp), or pAG in short. To avoid the background expression of P_{ant} due to the possible leakage, one more *antR* was inserted downstream of P_{ant}, resulting in pUC57-P_{ant}-*antR-antR-gfp* (4016 bp), or

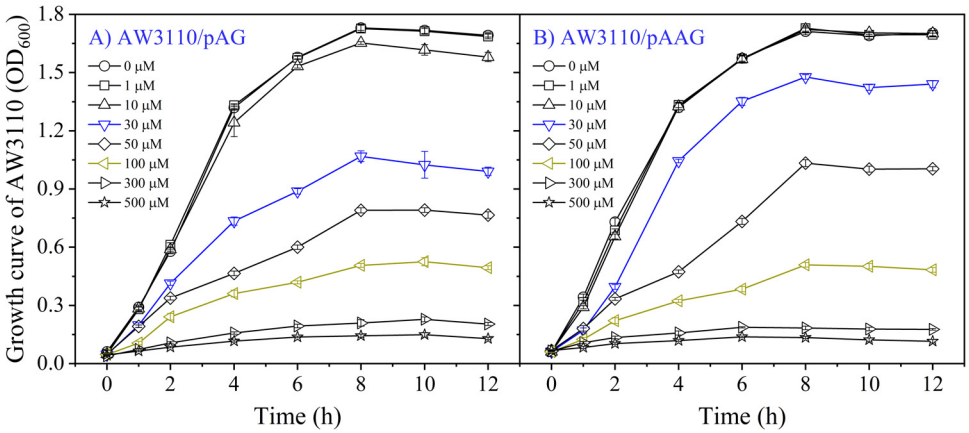

FIG 2 Growth curves of the strain AW3110/pAG (A) and AW3110/pAAG (B) at different concentrations of Sb(III).

pAAG in short (Fig. 1B). Thus, in the absence of inducer Sb(III), P_{ant} was firmly bound by expressed AntR, which effectively reduces promoter leakage.

To verify the successful construction of WCBs, the recombinant plasmids pAG and pAAG were isolated from the recombinant *E. coli* AW3110 strains and then identified by double digestion and sequencing. The gel electrophoresis resolved the identical size to the target fragments and the sequencing results further, suggesting that the construction of recombinant plasmids met the design goal (see Table S1 in the supplemental material).

To analyze the GFP fluorescence expressed by engineered strain AW3110, the cells were examined under a confocal microscope. As shown in Fig. S1 in the supplemental material, strain AW3110/pAAG exhibited an appreciable fluorescence upon Sb(III) addition. On the other hand, in the absence of Sb(III), a rather weak fluorescence signal was observed, suggesting the promoter leakage of the WCB. Notably, strain AW3110/pUC57 alone, as a control, presented no fluorescence signal. Moreover, to explore the relevance of the expression of GFP and the Sb(III) concentration, reverse transcriptase quantitative PCR (RT-qPCR) assays were performed to analyze the relative expression levels of GFP in the strains AW3110/pAAG with increasing Sb(III) concentrations. As shown in Fig. S2 in the supplemental material, the expression of GFP linearly correlated with Sb(III) concentration, indicating that the construction of WCB meets the design requirements.

The resistance of engineered strains to Sb(III). To determine an appropriate Sb (III) concentration range for evaluating the performance of WCBs, the Sb(III) resistance of engineered strains was investigated. Thus, the growth curves of strains AW3110/pAG and AW3110/pAAG were measured as a function of Sb(III) concentration. Figure 2 shows that the bacteria entered the logarithmic phase and the stationary phase of growth after incubation for about 1 and 8 h, respectively, at 37°C. In addition, the resistance of the two strains to >100 μM Sb(III) was not significantly different ($P = 0.2$ [100 μM], $P = 0.8$ [300 μM]), illustrating that AntR contributed little to the Sb(III) resistance. Moreover, as shown in Fig. S3 in the supplemental material, the resistance of strain AW3110/pAG to different Sb (III) concentrations had no obvious difference with AW3110/pUC57 ($P > 0.05$) (detailed in Table S2 in the supplemental material), suggesting that AntR may not play a major role in the Sb(III) resistance, which is in agreement with a previous study (18). In addition, no significant tolerance was observed when Sb(III) was <10 μM and Sb(III) was >100 μM, where the Sb (III) toxicity was pronounced and the cells barely grew (Fig. 2). Therefore, the concentration range of 0 to 100 μM was used to explore the response of WCBs to Sb(III).

Sensitivity and specificity. To examine the sensitivity, the WCBs AW3110/pAG and AW3110/pAAG were exposed to 0 to 100 μM Sb(III) for 2 h at 37°C. In the absence of Sb(III), the induction coefficient (IC) value of AW3110/pAAG (5.1 $\pm$ 0.1) was significantly lower than that of AW3110/pAG (8.6 $\pm$ 0.2), indicating that the double *antR* effectively alleviated the promoter leakage. As shown in Fig. 3, the linear dependence of IC on the logarithmic Sb(III) concentration started at 0.1 and 0.01 μM for AW3110/pAG and AW3110/pAAG,

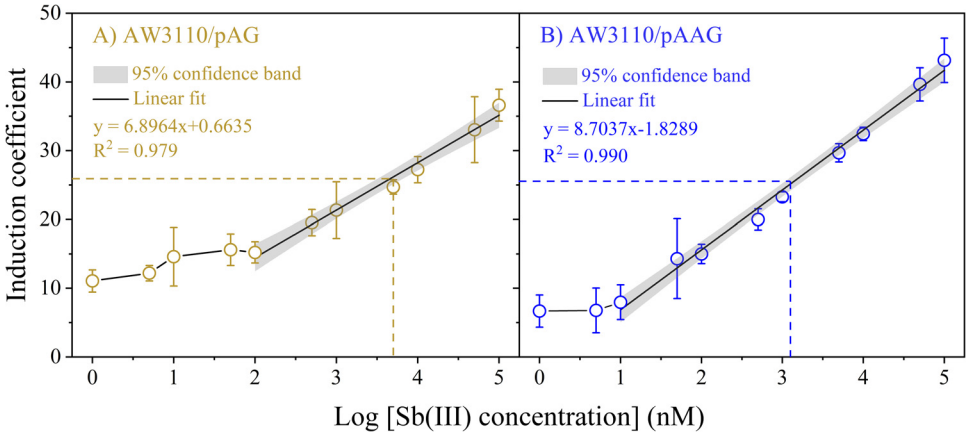

FIG 3 Concentration-dependent responses of the WCBs AW3110/pAG (A) and AW3110/pAAG (B) to 0 to 100 μM Sb(III). The dotted line indicates that the Sb(III) concentration reaches half of the maximum IC value. Error bars represent the standard deviation (n = 3).

respectively, suggesting that double *antR* enhanced the sensitivity by an order of magnitude. Meanwhile, the slope of the linear curve of AW3110/pAAG (8.7) is greater than that of AW3110/pAG (6.9) at a 95% confidence level, implying a more sensitive response. Moreover, the half-saturation Sb(III) that reaches the maximum IC was about 1 μM (log = 3) for pAAG and 5 μM (1og = 3.7) for pAG, emphasizing a better sensitivity for AW3110/pAAG again. Notably, AW3110/pAAG with the detection limit of 0.009 μM, as detailed in the supplemental material, is capable of measuring Sb for the WHO drinking water standard (0.05 μM or 6 μg/L).

To evaluate the specificity of the WCBs toward Sb(III), the interference from potential coexisting metals was examined, including As(III/V), Ca(II), Cd(II), Co(II), Cr(III), Cu(II), Fe(III), Mg(II), Mn(II), Ni(II), Pb(II), and Sb(V). As shown in Fig. 4, AW3110/pAAG exhibited a high IC value (>16) with 0.1 μM Sb(III), compared with the IC value at around 4.23 with 10 to 100 μM interfering metals. In addition, the IC values of the two WCBs did not fluctuate significantly in the concentration range of 0 to 100 μM, indicating that the WCBs did not respond to interfering metals. Notably, the IC value of AW3110/pAAG to interfering metals was much lower than that of AW3110/pAG (7 $\pm$ 1). To determine the effect of the *antR*

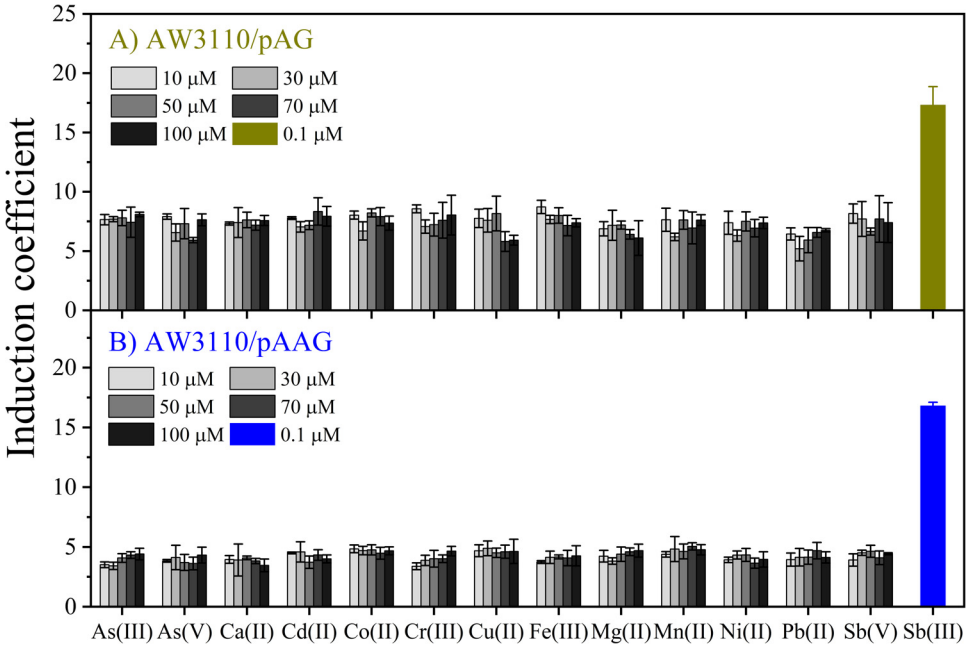

FIG 4 The specificity of the WCBs AW3110/pAG (A) and AW3110/pAAG (B) to Sb(III) (0.1 μM) and other potential coexisting ions (10 to 100 μM). Error bars represent the standard deviation (n = 3).

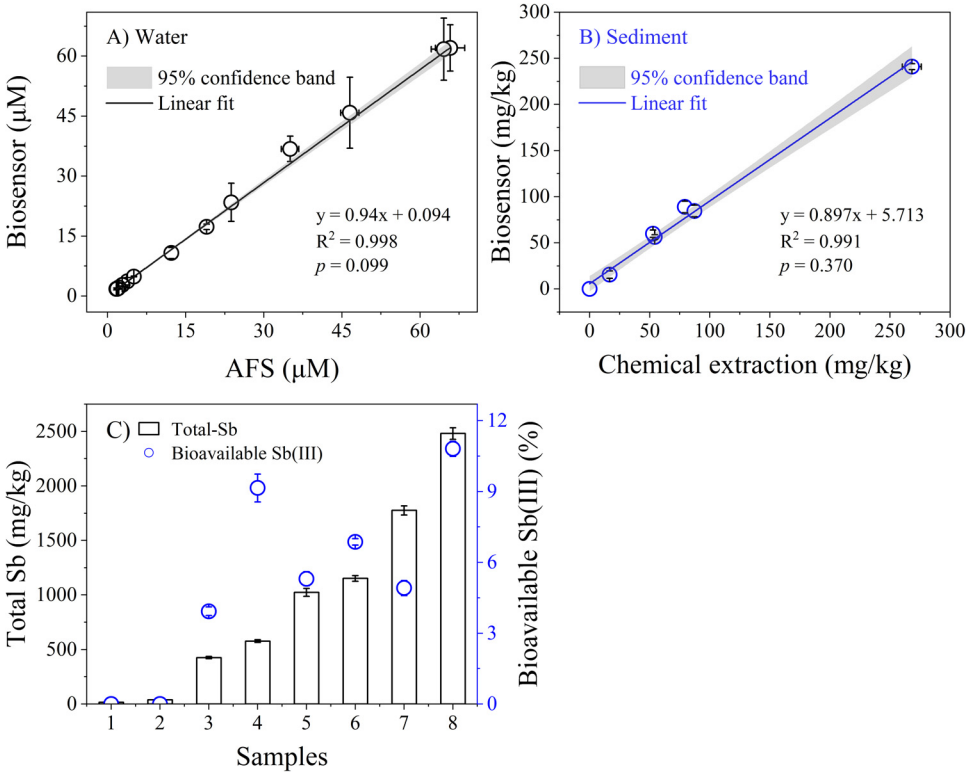

FIG 5 (A) Linear correlation between Sb(III) concentration of river water samples measured by the biosensor and AFS method. (B) Linear correlation between bioavailable Sb(III) in sediments extracted by the biosensor and chemical extraction method. (C) The total Sb concentration in sediments (vertical bars) and the percentage of bioavailable Sb (III) in total Sb (scatter). Error bars represent the standard deviation (n = 3).

addition on the specificity, the matched-sample t test was performed. As shown in Table S3 in the supplemental material, the IC values of AW3110/pAAG were significantly different from that of AW3110/pAG ($P < 0.05$), suggesting that by inserting an additional *antR* into the Sb(III) WCB, the background signal was diminished and the promoter leakage was alleviated.

Measuring bioavailable Sb(III) in environmental samples. To evaluate the application of AW3110/pAAG in the field, Sb(III) in 15 river water samples was analyzed, and the results were compared with high-pressure liquid chromatography-atomic fluorescence spectrometry (HPLC-AFS) (Fig. 5A). A linear correlation with a slope of 0.94 was obtained between WCB and AFS for Sb(III), ranging from 1.8 $\pm$ 0.3 to 62 $\pm$ 6 μM. In particular, no significant difference in Sb(III) concentrations was found by these two methods ($P = 0.1$), implying our WCB is capable of Sb(III) detection for aquatic samples.

To measure the bioavailable Sb(III) in sediments using WCB, the platform was constructed as shown in Fig. S4 in the supplemental material. Using a semipermeable membrane, the cells were separated from the suspension to facilitate the detection of fluorescent signals. Especially, the results of HPLC-AFS show that no significant difference existed in the Sb concentration inside and outside the semipermeable membrane ($P = 0.2$) (detailed in Table S4 in the supplemental material), confirming the feasibility of the detection system. The soluble Sb(III) fraction obtained by $MgCl_2$ extraction was defined as the bioavailable Sb(III) of sediments, representing the Sb(III) that entered the bacterial cells (20, 21). In addition, to determine the bioavailable Sb(III) concentration in sediments by WCB, the calibration curve was performed using 1 M $MgCl_2$ (see Fig. S5 in the supplemental material).

As shown in Fig. 5B, the bioavailable Sb(III) in eight sediment samples determined by the WCB exhibited no significant difference with the chemical extraction method ($P = 0.3$). In particular, the bioavailable Sb(III) (0 to 265 mg/kg of body weight) was much lower than the total Sb (0 to 2,450 mg/kg) (Fig. 5C). This finding is mainly because Sb(III) is readily complexed with natural organic materials or other macromolecules and the complexation may prevent

Sb from entering the cells (13). Thus, it has been well recognized that the bioavailable fraction is not necessarily equal to the dissolved fraction (22), which suggests that evaluating the available Sb(III) in sediments is more crucial for the accurate evaluation of Sb toxicity.

DISCUSSION

The toxicity of Sb(III) has garnered public attention and motivated recent research on Sb(III) monitoring. To assess the bioavailable Sb(III) of natural samples, the microbial-based whole-cell biosensors (WCBs) have attracted our attention. The research on arsenic (As)-WCBs showed that the discovery of the As(III)-specific binding protein ArsR was central to the construction of As-WCBs (12, 13). Due to the similar properties of Sb and As, an Sb biosensor was constructed based on the modification of the binding site of ArsR, but its specificity and sensitivity were insufficient (17). The lack of Sb(III) specific regulatory elements limited previous attempts at constructing Sb-specific WCBs. Recently, the transcriptional regulatory factor AntR that specifically recognizes Sb(III) has been reported (18, 19), which enabled the construction of Sb(III)-specific WCBs. Using the design of double *antR* insertion, we constructed a novel Sb (III) WCB AW3110/pAAG with a detection limit of 0.009 μM, which is sensitive enough to measure samples below the WHO maximum contaminant level of 0.05 μM Sb (Fig. 3 and 4). Thus, our study demonstrates the potential of AntR in the construction of WCB for Sb(III) analysis. However, to realize the progress of WCB from proof of concept to practical field applications, two main concerns need to be addressed.

One of the concerns is the promoter leakage commonly existed in WCBs (13, 14), which seriously lowers the sensitivity of WCBs. To address this issue, many attempts have been adopted, such as increasing transcriptional regulator binding sites (23), modifying ribosome-binding sites (24), and using a positive feedback signal amplifier (12). In this study, to alleviate the promoter leakage of Sb WCB, we inserted one more *antR* downstream of the Sb(III)-inducible promoter P_{ant} (see Fig. S6 in the supplemental material). In the absence of Sb(III), double copies of *antR* expressed more AntR protein to bind tightly to P_{ant}, thereby reducing the background expression (Fig. S6B). Notably, the detection limit of AW3110/pAAG (0.009 μM) was improved nearly 10 times compared with that of AW3110/pAG (0.091 μM), demonstrating that the additional regulatory gene is able to reduce promoter leakage (Fig. 3).

As shown in Fig. 4A, the promoter leakage also reduced the specificity of WCBs. Generally, the specificity may be improved by protein engineering to modify the interactions between the inducer Sb(III) in this study and the regulator (17, 25). A previous study on arsenic biosensors showed that a specific WCB was obtained by modulating the number and location of cysteines forming coordinative covalent bonds with arsenic species (26). By mutating Cys102 of the ArsR repressor to serine, a WCB with high selectivity for aromatic and trivalent methyl arsenic species was constructed (25). In our study, in addition to improving the sensitivity of WCBs, the insertion of an additional *antR* alleviated the promoter leakage and decreased its response to interference metals (Fig. 4B). Our AW3110/pAAG exhibited a high specificity toward Sb(III) compared with other metal ions at 3 orders of magnitude higher concentrations.

Another concern of WCBs is that the interference of the complex environmental matrix hinders the actual environment application. Only a fraction of Sb(III) in soils and sediments is soluble and termed the bioavailable fraction (10, 11). The WCBs based on the biological stress response mechanism of viable cells have been used to measure metal bioavailability (11, 25). However, colloidal particles may interfere with the fluorescence and optical density at 600 nm (OD_{600}) signals due to their strong refraction and absorption of light (26, 27). Here, we used a semipermeable membrane to separate the biosensor bacteria from the suspension (Fig. S4). Notably, the concentration of bioavailable Sb(III) in sediments measured by WCB existed with no significant difference from the chemical extraction method ($P = 0.4$) (Fig. 5B). Thus, the microbial-based WCBs effectively reflect the bioavailable Sb(III), which is of great importance for evaluating Sb(III) exposure. Moreover, freeze-dried bacteria were prepared, making these WCBs reagent like. The activity of the cells was recovered in about 30 min (see Fig. S7 in the supplemental material), enabling the convenient use of WCBs in the field.

TABLE 1 Sequences of oligonucleotide primers used in this work[a]

Name	Sequence (5′–3′)	Target
ant-F	GCTGGCCTTTTGCTCACATGTTCCCTGGCGTGCATGGCA	Construction of pAG
ant-R	AAAGCCATTTATCCGCCAGCTTGCTGTT	Construction of pAG
gfp-F	TTGGCGGATAAATGTCGAAGGGCGAGGAGC	Construction of pAG
gfp-R	GTACTGAGAGTGCACCATATGCTACTTGTACAGCTCGTCCATGCC	Construction of pAG
ant-F	GCTGGCCTTTTGCTCACATGTTCCCTGGCGTGCATGGCA	Construction of pAAG
ant-R	AAAGCCATTTATCCGCCAGCTTGCTGTT	Construction of pAAG
antR-F	GCTGGCGGATAAATGGCTTTAGAAAAGAGAAATGAACTAC	Construction of pAAG
antR-R	CGCCCTTCGACATCATGATTACGCCAAGCTTTTATCC	Construction of pAAG
gfp-F	AATCATGATGTCGAAGGGCGAGGAGC	Construction of pAAG
gfp-R	GTACTGAGAGTGCACCATATGCTACTTGTACAGCTCGTCCATGCC	Construction of pAAG
YZ-F	AGCAACGCGGCCTTTTTACG	Verification of pAG or pAAG
YZ-R	GCGCGTTTCGGTGATGACGG	Verification of pAG or pAAG
gfp-F	ATGTCGAAGGGCGAGGAGCT	Used for RT-qPCR
gfp-R	CTACTTGTACAGCTCGTCCA	Used for RT-qPCR
16S-F	CAAGGGCACAACCTCCAAGT	Used for RT-qPCR
16S-R	TGTAGCGGTGAAATGCGTAG	Used for RT-qPCR

[a]Restriction enzyme cutting sites are underlined.

In conclusion, this study provides the first whole-cell biosensor for bioavailable Sb (III) detection and demonstrates the importance of inserting one more regulatory gene to prevent promoter leakage and to improve the sensitivity of WCB.

MATERIALS AND METHODS

Strain, plasmid, and reagents. *Escherichia coli* AW3110 is the *arsRBC* deletion mutant of *E. coli* W3110 (28, 29). To eliminate the interference of endogenous *arsR*, strain AW3110 was used for gene cloning and as the host of whole-cell biosensors (WCBs). The *antR* (WP_034375793) gene and its promoter (P_{ant}) from *Comamonas testosterone* JL40 were chemically synthesized, codon optimized, and cloned into pUC57, generating plasmid pUC57-*antR* (Sangon Biotech, Shanghai, China). The plasmid pCDFDuet-1 was purchased from Sangon and used to obtain the *gfp* gene. The pUC57 plasmid was used to construct recombinant plasmids to carry the Sb(III) transcriptional repressors (*antR*), its cognate promoters (P_{ant}), and reporter gene *gfp*.

All reagents are of analytical grade and were obtained from commercial sources, which were detailed in the supplemental material. The Luria-Bertani (LB) medium was used to aerobically incubate engineering bacteria, and its specific components are shown in the supplemental material. The solid plates needed an additional 1.5% (wt/vol) agar and were supplemented with 100 μg/mL of ampicillin (Amp^+) for selecting positive colonies. PCR reagents were purchased from Mei5 Biotechnology, Co., Ltd. (Beijing, China).

Construction of the sensor plasmids. The recombinant plasmids were constructed using the homologous recombination method. In detail, the linear vector pUC57 was first constructed by restriction endonucleases NdeI and PciI (New England BioLabs, Beijing, China). Then, the P_{ant} (192 bp), *antR* (375 bp), and *gfp* (717 bp) fragments were amplified separately using the plasmids pUC57-*antR* and pCDFDuet-1 as the template. Finally, the linear vector pUC57 and the obtained fragments were assembled by the ClonExpress Ultra one-step cloning kit C115 (Vazyme, Nanjing, China). The reporter *gfp* was under the control of the promoter P_{ant} in vector plasmid pUC57, generating plasmid pUC57-P_{ant}-*antR*-*gfp*. All constructs were confirmed by double digestion/gel electrophoresis and Sanger sequencing by TsingKe (Beijing, China). The primers designed for PCR amplification or plasmid verification were listed in Table 1 and were chemically synthesized by TsingKe.

To further explore the fluorescence properties of GFP expressed by engineered strains, strains AW3110/pAG and AW3110/pAAG with or without Sb(III) treatment were observed under a confocal microscope. The confocal images of the strain AW3110/pUC57 under the same conditions were served as the black. Confocal imaging was performed using a Leica SP5 confocal laser scanning microscopy (German) with fluorescence mode under an excitation of 405 nm and emission wavelength of 410 to 700 nm. To explore the relevance between the expression of GFP and the Sb(III) concentration, the RNA of strains AW3110/pAAG with 0 to 100 μM Sb(III) was extracted, and RT-qPCR was carried out (5). The information on primers is shown in Table 1. A detailed description of RNA extraction and RT-qPCR is shown in the supplemental material.

Growth curve of the WCB strains. To determine the Sb(III) concentration range for studying the performance of WCBs, the toxic effect of Sb(III) on engineered strains needs to be clarified. Strains AW3110/pAG and AW3110/pAAG were grown overnight in LB medium containing 100 μg/mL of Amp^+ at 37°C with shaking at 200 rpm. The optical density at 600 nm (OD_{600}) of the cultures was adjusted to 2.0 using fresh LB medium, and 0.5-mL cultures were transferred to 50 mL fresh medium containing Sb(III) with different final concentrations (from 0 to 500 μM). Then the strains were incubated at 37°C with shaking at 200 rpm, and the growth of strains was monitored periodically by OD_{600} using a UV spectrophotometer (DR 2800; Hach, China).

Evaluation of the sensitivity and specificity of WCBs. To evaluate the sensitivity and specificity of WCBs, 3 mL of the overnight cultures, with an OD_{600} adjusted to 1.2, was added to 3 mL of ion solution. The Sb (III) and potential interfering ions, such as As(III/V), Ca(II), Cd(II), Co(II), Cr(III), Cu(II), Fe(III), Mg(II), Mn(II), Ni(II), Pb(II), and Sb(V), were added separately at a specific concentration. The incubation experiments were conducted for 2 h at 37°C with shaking at 200 rpm, and then the OD_{600} was monitored. The relative fluorescence unit (RFU)

was measured by an Edinburgh FLS1000 spectrofluorometer system equipped with a temperature-control component (Oxford microstatDN) with an excitation/emission of 450/530 nm. All experiments were performed in triplicate, and the *E. coli* AW3110/pUC57 exposed noninducer was used as the negative control.

The induction coefficient (IC) was calculated and used to present the fluorescent intensity (12), as follows: IC = AFU/BFU, where the arbitrary fluorescence unit (AFU) is defined as the RFU divided by the OD_{600} at specific Sb(III) concentrations. The background fluorescence unit (BFU) is defined as the RFU of AW3110/pUC57 culture without metal ions divided by its OD_{600}. A linear correlation between the Sb(III) concentrations and the IC values was performed to analyze the sensitivity of WCBs. The matched-sample *t* test was performed to analyze possible significant differences in specificity between AW3110/pAG and AW3110/pAAG.

Measurement of real environmental samples. To evaluate the application potential of the WCB in the real environment, the Sb(III) concentrations of 15 river water samples were tested by WCB and AFS, respectively. A total of 3 mL of river sample was mixed with 3 mL of overnight cultures, and the OD_{600} value was adjusted to 1.2. The culture was incubated for 2 h at 37°C with shaking at 200 rpm, and then the OD_{600} and the RFU of strains were measured. To verify the results of the WCB analysis, the Sb(III) concentration of real samples was certified by the HPLC-AFS standard method. The experiment details of the HPLC-AFS are described in the supplemental material.

To realize the convenience of using WCBs in the real field, freeze-dried bacteria were prepared using skim milk as a protectant. Furthermore, the reconstitution time of the freeze-dried bacteria was determined using the incubation experiments. The details of freeze-dried bacterial preparation and reconstitution are shown in the supplemental material. Briefly, the freeze-dried bacteria (OD_{600}, 0.6) were suspended in 20 mL of LB medium to restore for 30 min at room temperature without shaking. Then, the cultures were packed in a semipermeable membrane (MD34-7000; Vake, USA) to prepare the tea bags.

To measure the bioavailable Sb(III) in sediments using WCBs, the detection system was constructed, as shown in Fig. S4. Using a semipermeable membrane as a tea-bag design, WCB bacteria can be separated from suspension to facilitate the detection of fluorescent signals. The sediment was first suspended in 100 mL of a 1 M $MgCl_2$ solution at a ratio of 1:100 to extract the bioavailable Sb(III) (20, 21). Then, the tea bag was immersed in the extraction solution. After 2 h, the OD_{600} value and the fluorescence intensity of bacteria were detected to evaluate the Sb(III) bioavailability. Following the same process, the calibration curve was performed in the range of 0 to 100 μM Sb(III) in 1 M $MgCl_2$ to determine the Sb(III) concentration in sediments by WCB. To verify the results of the WCB analysis, the Sb(III) concentration in the extraction solution was certified by the HPLC-AFS standard method. The sediments used in the study are described in our previous work (21). The details of all environmental samples to be tested are listed in Table S5 and S6 in the supplemental material.

Statistical analysis. The statistical analysis was carried out using the software IBM SPSS Statistics 22. The correlation analysis between two different elements was conducted. The independent-sample *t* test or the matched-sample *t* test was performed to ascertain possible significant differences between the AW3110/pAG and AW3110/pAAG groups. The method of minimizing the residual sum of squares was used to estimate the Sb(III) concentration range of the quantitative calibration curve of the biosensor (30). Significance was considered when the *P* value was <0.05.

Data availability. All data are shown here and in the supplemental material. The NCBI accession number of *antR* from *C. testosterone* JL40 is WP_034375793. All plasmids and strains used in the study will be available by the corresponding author upon request.

SUPPLEMENTAL MATERIAL

Supplemental material is available online only.

SUPPLEMENTAL FILE 1, PDF file, 0.7 MB.

ACKNOWLEDGMENTS

This work was supported by the National Natural Science Foundation of China (42230706 and 42207440), the National Basic Research Program of China (2022YFC3701302), and the Shandong Province Natural Science Foundation of Major Basic Research Program, China (ZR2020ZD34).

L.Z., Conceptualization, Methodology, Analyzed Data, Formal Analysis, Investigation, Writing – Original Draft; L.Y., Writing – Review & Editing; C.J., Conceptualization, Methodology, Supervision, Writing – Review & Editing.

We declare that we have no known competing financial interests or personal relationships that could have appeared to influence the work reported in this paper.

REFERENCES

1. Ye L, Qiu SX, Li XH, Jiang YX, Jing CY. 2018. Antimony exposure and speciation in human biomarkers near an active mining area in Hunan, China. Sci Total Environ 640–641:1–8. https://doi.org/10.1016/j.scitotenv.2018.05.267.
2. Li J, Wang Q, Oremland RS, Kulp TR, Rensing C, Wang G. 2016. Microbial antimony biogeochemistry: enzymes, regulation, and related metabolic pathways. Appl Environ Microbiol 82:5482–5495. https://doi.org/10.1128/AEM.01375-16.
3. Filella M, Belzile N, Lett MC. 2007. Antimony in the environment: a review focused on natural waters. III. Microbiota relevant interactions. Earth Sci Rev 80:195–217. https://doi.org/10.1016/j.earscirev.2006.09.003.
4. Ye L, Meng XG, Jing CY. 2020. Influence of sulfur on the mobility of arsenic and antimony during oxic-anoxic cycles: differences and competition. Geochem Cosmochim Acta 288:51–67. https://doi.org/10.1016/j.gca.2020.08.007.

5. Zhang LX, Ye L, Yin ZP, Xiao K, Jing CY. 2021. Mechanistic study of antimonate reduction by *Escherichia coli* W3110. Environ Pollut 291:118258. https://doi.org/10.1016/j.envpol.2021.118258.
6. Wang LY, Ye L, Yin ZP, Zhang LX, Jing CY. 2022. Antimonite oxidation by microbial extracellular superoxide in *Pseudomonas* sp. SbB1. Geochem Cosmochim Acta 316:122–134. https://doi.org/10.1016/j.gca.2021.10.019.
7. Kale GM, Davidson AJ, Fray DJ. 1996. Solid-state sensor for measuring antimony in non-ferrous metals. Solid State Ion 86–88:1101–1105. https://doi.org/10.1016/0167-2738(96)00276-7.
8. Yu YQ, Du JJ, Chan TS, Jing CY. 2020. Core-shell AuFe@FeO_x-CFC as electrochemical sensor for trace antimony analysis. Sens Actuators B Chem 319:128322. https://doi.org/10.1016/j.snb.2020.128322.
9. Berlina AN, Komova NS, Zherdev AV, Gaur MS, Dzantiev BB. 2019. Colorimetric technique for antimony detection based on the use of gold nanoparticles conjugated with poly-A oligonucleotide. Appl Sci-Basel 9:4782. https://doi.org/10.3390/app9224782.
10. Mimee M, Nadeau P, Hayward A, Carim S, Flanagan S, Jerger L, Collins J, McDonnell S, Swartwout R, Citorik RJ, Bulovic V, Langer R, Traverso G, Chandrakasan AP, Lu TK. 2018. An ingestible bacterial-electronic system to monitor gastrointestinal health. Science 360:915–918. https://doi.org/10.1126/science.aas9315.
11. van der Meer JR, Belkin S. 2010. Where microbiology meets microengineering: design and applications of reporter bacteria. Nat Rev Microbiol 8:511–522. https://doi.org/10.1038/nrmicro2392.
12. Jia XQ, Bu RR, Zhao TT, Wu K. 2019. Sensitive and specific whole-cell biosensor for arsenic detection. Appl Environ Microbiol 85:e00694-19. https://doi.org/10.1128/AEM.00694-19.
13. Kaur H, Kumar R, Babu JN, Mittal S. 2015. Advances in arsenic biosensor development—a comprehensive review. Biosens Bioelectron 63:533–545. https://doi.org/10.1016/j.bios.2014.08.003.
14. Dieudonne A, Preveral S, Pignol D. 2020. A sensitive magnetic arsenite-specific biosensor hosted in magnetotactic bacteria. Appl Environ Microbiol 86:e00803-20. https://doi.org/10.1128/AEM.00803-20.
15. Hansen ML, He ZM, Wibowo M, Jelsbak L. 2021. A whole-cell biosensor for detection of 2,4-diacetylphloroglucinol (DAPG)-producing bacteria from grassland soil. Appl Environ Microbiol 87:e01400-20. https://doi.org/10.1128/AEM.01400-20.
16. Wan XY, Volpetti F, Petrova E, French C, Maerkl SJ, Wang BJ. 2019. Cascaded amplifying circuits enable ultrasensitive cellular sensors for toxic metals. Nat Chem Biol 15:540–548. https://doi.org/10.1038/s41589-019-0244-3.
17. Lee W, Kim H, Jang G, Kim BG, Yoon Y. 2020. Antimony sensing whole-cell bioreporters derived from ArsR genetic engineering. Appl Microbiol Biotechnol 104:2691–2699. https://doi.org/10.1007/s00253-020-10413-5.
18. An LJ, Luo X, Wu MH, Feng LL, Shi KX, Wang GJ, Rosen BP, Li MS. 2021. *Comamonas testosteroni antA* encodes an antimonite-translocating P-type ATPase. Sci Total Environ 754:142393. https://doi.org/10.1016/j.scitotenv.2020.142393.
19. Viswanathan T, Chen J, Wu MH, An LJ, Kandavelu P, Sankaran B, Radhakrishnan M, Li MS, Rosen BP. 2021. Functional and structural characterization of AntR, an Sb(III) responsive transcriptional repressor. Mol Microbiol 116:427–437. https://doi.org/10.1111/mmi.14721.
20. Keon NE, Swartz CH, Brabander DJ, Harvey CF, Hemond HF. 2001. Validation of an arsenic sequential extraction method for evaluating mobility in sediments. Environ Sci Technol 35:2778–2784. https://doi.org/10.1021/es001511o.
21. Zhang D, Guo JL, Xie XJ, Zhang YH, Jing CY. 2022. Acidity-dependent mobilization of antimony and arsenic in sediments near a mining area. J Hazard Mater 426:127790. https://doi.org/10.1016/j.jhazmat.2021.127790.
22. Lindfors S, Osterlund H, Lundy L, Viklander M. 2021. Evaluation of measured dissolved and bio-met predicted bioavailable Cu, Ni and Zn concentrations in runoff from three urban catchments. J Environ Manage 287:112263. https://doi.org/10.1016/j.jenvman.2021.112263.
23. Stocker J, Balluch D, Gsell M, Harms H, Feliciano J, Daunert S, Malik KA, Van der Meer JR. 2003. Development of a set of simple bacterial biosensors for quantitative and rapid measurements of arsenite and arsenate in potable water. Environ Sci Technol 37:4743–4750. https://doi.org/10.1021/es034258b.
24. Wackwitz A, Harms H, Chatzinotas A, Breuer U, Vogne C, van der Meer JR. 2008. Internal arsenite bioassay calibration using multiple bioreporter cell lines. Microb Biotechnol 1:149–157. https://doi.org/10.1111/j.1751-7915.2007.00011.x.
25. Yoon Y, Kim S, Chae Y, Jeong SW, An YJ. 2016. Evaluation of bioavailable arsenic and remediation performance using a whole-cell bioreporter. Sci Total Environ 547:125–131. https://doi.org/10.1016/j.scitotenv.2015.12.141.
26. Calderon FJ, Reeves JB, III, Collins HP, Paul EA. 2011. Chemical differences in soil organic matter fractions determined by diffuse-reflectance mid-infrared spectroscopy. Soil Sci Soc Am J 75:568–579. https://doi.org/10.2136/sssaj2009.0375.
27. Zeng Y, Fang G, Fu Q, Peng F, Wang X, Dionysiou DD, Guo J, Gao J, Zhou D, Wang Y. 2022. Mechanistic study of the effects of agricultural amendments on photochemical processes in paddy water during rice growth. Environ Sci Technol 56:4221–4230. https://doi.org/10.1021/acs.est.2c00145.
28. Zhang J, Cao TT, Tang Z, Shen QR, Rosen BP, Zhao FJ. 2015. Arsenic methylation and volatilization by arsenite S-adenosylmethionine methyltransferase in *Pseudomonas alcaligenes* NBRC14159. Appl Environ Microbiol 81:2852–2860. https://doi.org/10.1128/AEM.03804-14.
29. Yan Y, Xue XM, Guo YQ, Zhu YG, Ye J. 2017. Co-expression of cyanobacterial genes for arsenic methylation and demethylation in *Escherichia coli* offers insights into arsenic resistance. Front Microbiol 8:60. https://doi.org/10.3389/fmicb.2017.00060.
30. Liu J, Wu SY, Zidek JV. 1997. On segmented multivariate regression. Stat Sin 7:497–525.